Inorganic Chemistry

Communication

pubs.acs.org/IC

Two Isostructural 3D Lanthanide Coordination Networks (Ln = Gd^{3+}, Dy^{3+}) with Squashed Cuboid-Type Nanoscopic Cages Showing Significant Cryogenic Magnetic Refrigeration and Slow Magnetic Relaxation

Soumava Biswas, Himanshu Sekhar Jena, Amit Adhikary, and Sanjit Konar*

Department of Chemistry, IISER Bhopal, Bhopal 462066, India

Supporting Information

ABSTRACT: Two isostructural lanthanide-based 3D coordination networks [Ln = Gd^{3+} (**1**), Dy^{3+}(**2**)] with densely packed distorted cuboid nanoscopic cages are reported for the first time. Magnetic characterization reveals that complex **1** shows a significant cryogenic magnetocaloric effect ($-\Delta S_m$ = 44 J kg^{-1} K^{-1}), whereas **2** shows slow relaxation of magnetization.

Lanthanide-based molecular magnetic materials are a forefront area of research owing to their proposed applications in future devices like molecular magnets,[1] magnetic refrigerants,[2] etc. Magnetic refrigeration happens because of a phenomenon known as the magnetocaloric effect (MCE), and the magnitude of the MCE of a magnetic material is characterized by ΔS_m, the isothermal magnetic entropy change, and ΔT_{ad}, the adiabatic temperature change following a change in the applied magnetic field. Gadolinium is often present in magnetic refrigerant materials because of its large spin ground state, quenched orbital momentum, and weak superexchange interactions.[3] To date, some impressive gadolinium-based compounds associated with molecular magnetic cooling have been reported.[4] However, the controlled and long-range dense spatial assembly of the Gd^{3+} spin centers is vital for the design of an ideal magnetic refrigerant, and therefore higher-dimensional coordination polymers should also play an important role. The magnetic density can also be maximized by, for example, limiting the amount of nonmagnetic elements, which act passively in the physical process. Therefore, the small size of the ligands should be preferable. On the other hand, the intrinsic magnetic anisotropy and the increased number of unpaired f electrons of dysprosium may be responsible for the large energy barrier for reversal of magnetization, especially when combined with suitable ligands.

The present work stems from our earlier investigation of the MCE on a gadolinium squarate 2D coordination polymer,[5a] and a high-symmetry 3D iron(II)-based squashed cuboctahedral nanoscopic cage behaves like a spin-canting antiferromagnet.[5b] Herein we report the synthesis, characterization, and magnetic property investigation of two heteroleptic isostructural lanthanide-based 3D coordination networks $[Ln(C_4O_4)(C_2O_2)_{0.5}(H_2O)_2]_n$ [Ln = Gd^{3+} (**1**) and Dy^{3+} (**2**)]. Structural investigations reveal that the 3D framework consists of extended cuboid nanoscopic cages. Magnetic characterizations show that complex **1** acts as an efficient cryogenic magnetic refrigerant ($-\Delta S_m$ = 44 J kg^{-1} K^{-1}), whereas **2** shows slow relaxation of magnetization. Because complexes **1** and **2** are isostructural in nature, the structural description of complex **1** has been illustrated with suitable comparison with complex **2**.

Both of the complexes were crystallized in space group $P2_1/c$, and the relevant structural refinement parameters are listed in Table S1 in the Supporting Information (SI). The asymmetric unit of complex **1**, $[Ln(C_4O_4)(C_2O_4)_{0.5}(H_2O)_2]$, contains one Gd^{3+} ion, one squarate, half of the oxalate ligand, and two coordinated water molecules (Figure S1a in the SI). Each lanthanide center is eight-coordinated with four oxygen atoms from four squarate ligands, two oxygen atoms from one oxalate ligand, and two other oxygen atoms from coordinated water molecules. Thus, the coordination geometry around the gadolinium centers can be described as a distorted square-antiprismatic (Figure S1b in the SI). The relevant bond parameters around the lanthanide centers in complexes **1** and **2** are listed in Table S2 in the SI and are found to be in the range of reported analogues of a Tb^{3+}-based 3D framework containing similar set of ligands.[6] It can be seen that each squarate ion acts as a tetradentate ligand (μ_4-connected) and binds four lanthanide ions to form lanthanide rectangles (Figure 1a). Four lanthanide rectangles are face-shared by a common squarate ion and result in

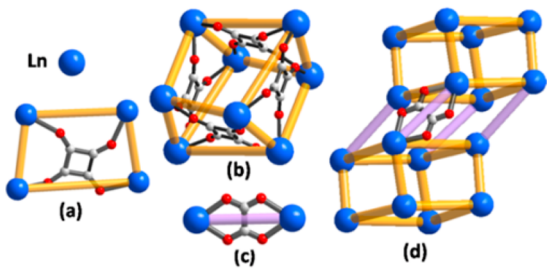

Figure 1. Schematic representations of (a) the bridging mode of a squarate ion, (b) a distorted lanthanide cuboid nanocage showing four close faces by squarate ligands and two open faces, (c) the bridging mode of an oxalate ion, and (d) two adjacent cuboid nanocages connected by an oxalate ion, which closes the open face of each cuboid. Color code: Ln, blue; O, red; C, gray; squarate bridge, yellow rod; oxalate bridge, pink.

Received: December 10, 2013
Published: April 1, 2014

   dx.doi.org/10.1021/ic4030316 | *Inorg. Chem.* 2014, 53, 3926−3928

a distorted lanthanide cuboid cage by joining eight lanthanide ions thru imaginary lines (Figure 1b). "Cuboid" is one out of five "Platonic Solids" having 6 faces, 8 vertices, and 12 edges.[7] Thus, in **1**, out of six faces, four are occupied by four squarate ions and two opposite faces remains open. The vertices of the cuboids are occupied by eight lanthanide ions. The distances between two opposite faces of the cuboids are ~6.3 and ~7.8 Å for **1** and **2**, respectively, as calculated by the distance between the centroids of two squarate ions in opposite faces. The distances between two lanthanide centers along the edges are ~6.2 and ~7.6 Å for **1** and **2**, respectively. The cuboids are "homoleptic" in nature because they contain only a single ligand, i.e., a squarate ion. Each adjacent cuboid shares a common face and is extended to form a homoleptic 2D coordination framework, as shown in Figure S2a in the SI, and its skeletal view is shown in Figure S2b in the SI.

However, it is surprising to note that the two open faces of the squarate-bridged lanthanide cuboids are closed by bis(bidentate) oxalate ions (Figure 1c) and form a "heteroleptic" lanthanide cuboid (Figure 1d). Hence, two adjacent homoleptic 2D lanthanide bilayers are connected by bis(bidentate) oxalate ions to form a 3D coordination network, as shown in (Figure 2a),

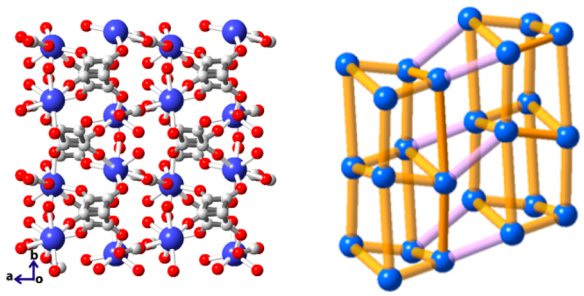

Figure 2. (a) 3D packing diagram of **1** down the *c* axis illustrating the bridging modes of oxalate ions in the assembly of 2D lanthanide cuboid nanocages and (b) its skeletal view. Color codes are the same as those in Figure 1

and its skeletal view is represented in Figure 2b. Thus, the orientation of the oxalate ions in the 3D framework restricts the entrance and exit of external guests (anions, gases, or vapors) inside the framework, and that was further confirmed by *PLATON* analysis[8] because no solvent-accessible void was found. A polyhedral view of complex **1** along the *a* axis is illustrated in Figure S3 in the SI. Overall, the network topology of **1** can be best described as a 3D binodal 4,5-connected net with a Schälfli symbol of $\{4^2.6^2.8^2\}\{4^6.6^4\}$, as calculated by TOPOS analysis.[9] This network is identified by a "xah" topological type (Figure S4 in the SI) in Reticular Chemistry Structure Resource database.

The direct-current (dc) magnetic susceptibility data for **1** and **2** were collected at 1000 Oe in the temperature range of 1.8−300 K (Figure S5 in the SI). The room temperature $\chi_M T$ (χ_M = molar magnetic susceptibility) values of **1** and **2** are 7.39 and 13.67 cm^3 $K\,mol^{-1}$, respectively. For complex **1**, the room temperature $\chi_M T$ is well consistent with the expected spin-only $\chi_M T$ value [7.81 cm^3 $K\,mol^{-1}$ for one Gd^{3+} ($^8S_{7/2}$ and g = 1.99)]. This small difference is due to the presence of dominant antiferromagnetic interaction between the adjacent Gd^{3+}. The molar magnetic susceptibility data of **1** were fitted according to the Curie−Weiss equation, $\chi_M = C/(T - \theta)$, which afforded the Curie constants (C) = 7.41 cm^3 $K\,mol^{-1}$ and Weiss constants (θ) = −0.18 K for complex **1**. For complex **2**, the expected room temperature $\chi_M T$ value [14.18 cm^3 $K\,mol^{-1}$ for one Dy^{3+} ($^6H_{15/2}$ and g = 1.33)] is higher than the spin-only value due to orbital contribution. The shape of the susceptibility curves for complexes **1** and **2** indicates the presence of a dominant antiferromagnetic interaction between adjacent metal centers in both complexes. Magnetization data for complex **1** were measured in the temperature range of 2−10 K (Figure S6a in the SI), which shows a steady increase with increasing field (H) and saturation values of 6.93 $N\mu_B$ at 7 T and 2 K. However, **2** does not show complete saturation even at the highest field measured, 7 T, and at 2 K. This may be due to the high magnetic anisotropy present in Dy^{3+} ions (Figure S6b in the SI). The magnetization value reaches up to 5.11 $N\mu_B$ for **2**. For complex **2**, the plot of $M/N\mu_B$ versus H/T (Figure S7 in the SI) shows that all isotherm magnetization curves do not collapse on the same master curve, further indicating the anisotropic nature of the Dy^{3+} ions.[10]

Taking the low M_w/N_{Gd} ratio (where the molecular mass is M_w = 349.33 g mol^{-1} and N_{Gd} = number of gadolinium ions present per mole of complex **1**) of 349.33 into account, complex **1** can be considered as a dense magnetic material, which, in turn, might be a good candidate for cryogenic magnetic refrigeration. The magnetic entropy change ΔS_m for complex **1** is calculated from the magnetization data using the Maxwell relation $\Delta S_m(T) = \int[\partial M(T,H)/\partial T]_H\, dH$.[11] Theoretically, the full entropy change per mole of Gd^{3+} ion is 17.3 J mol^{-1} K^{-1}, as calculated from the equation $R\ln(2S + 1)$, where $S = {}^7/_2$. So, the calculated value of the entropy change from complex **1** is 49.52 J kg^{-1} K^{-1}. The experimental obtained $-\Delta S_m$ value at 3 K for ΔH = 7 T (44.0 J kg^{-1} K^{-1}; Figure 3) is found to be large, however, comparable

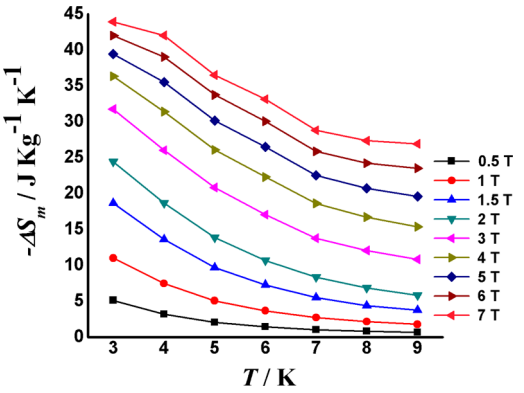

Figure 3. ΔS_m calculated by using the magnetization data of complex **1** at different fields (H) and temperatures (T).

with a few reported gadolinium-based 3D metal−organic frameworks (MOFs) having a maximum entropy above 40 J kg^{-1} K^{-1} ($[Gd(HCOOH)_3]$, 55.9 J kg^{-1} K^{-1}),[4n] ($\{[Gd_6(\mu_6\text{-}O)(\mu_3\text{-}OH)_8(\mu_4\text{-}ClO_4)_4(H_2O)_6](OH)_4\}_n$, 46.6 J kg^{-1} K^{-1}),[4g] ($[Gd_6(OH)_8(suc)_5(H_2O)_2]\cdot 2H_2O$, 48.0 J kg^{-1} K^{-1}),[4j] ($[Gd(HCOO)(C_8H_4O_4)]_n$, 47 J kg^{-1} K^{-1}),[4d] etc. The calculated volumetric entropy change for complex **1** of 127.6 mJ cm^{-3} K^{-1} is also very high considering the other examples available in the literature (Table S4 in the SI).

To inspect the magnetic dynamics of **2**, the frequency and temperature dependencies of the alternating-current (ac) susceptibilities were collected under different dc fields and a 3.5 Oe ac magnetic field. The out-of-phase frequency-dependent signals were obtained at different fields. However, because of the fast quantum tunnelling of magnetization (QTM),[1b] maxima of the out-of-phase ac susceptibility signals were absent for ac measurement at zero dc field (Figure S8 in the SI). Therefore, in

dx.doi.org/10.1021/ic4030316 | Inorg. Chem. 2014, 53, 3926−3928

order to suppress the QTM, ac measurements were performed at different dc fields (Figure S9 in the SI). At 1800 Oe, maxima were observed for both out-of-phase and in-phase ac susceptibilities. Although maxima for in-phase ac susceptibility are frequency-independent, frequency-dependent out-of-phase susceptibility confirms the presence of slow relaxation of magnetization. At a higher field of 3500 Oe, maxima for out-of-phase ac susceptibility disappeared (Figure S10b in the SI). So, from peak maxima of out-of-phase ac susceptibilities at an optimized dc field of 1800 Oe (Figure S9b), we plot $\ln(1/\tau)$ versus $1/T$ using the Arrhenius equation

$$1/\tau = \frac{1}{\tau_0}\exp\left(\frac{-U_{\text{eff}}}{kT}\right) \quad (1)$$

where U_{eff} is the effective anisotropic energy barrier, k is the Boltzmann constant, and $1/\tau_0$ is the preexponential factor. The least-squares fit to eq 1, shown as a solid line (Figure S11 in the SI), afforded the significant energy barrier of U_{eff} = 10.8 K for thermal relaxation and the relaxation time $\tau_0 = 2.0 \times 10^{-6}$ s, which is consistent with the expected characteristic relaxation time 10^{-6}–10^{-11} s for single-molecule magnets and other dysprosium-based MOFs.[1,12] The Cole–Cole plot is shown in Figure S12 in the SI, as evidence of the slow magnetic relaxation processes occurring in complex **2**.[12a]

In summary, we have illustrated the synthesis of two isostructural 3D MOFs with squashed nanoscopic cuboid-type cages. The aesthetically important structural feature in the complexes is the presence of a special array of metal centers in 3D space. In addition to the fascinating structural features, complexes reveal interesting magnetic properties as an efficient cryogenic magnetic refrigerant and molecular magnet.

■ ASSOCIATED CONTENT

Supporting Information

X-ray crystallographic data in CIF format, synthetic details, materials and method, structural figures, PXRD and TGA plots, magnetic plots and crystallographic table, tables containing bond distances and angles, and hydrogen-bonding parameters. This material is available free of charge via the Internet at http://pubs.acs.org.

■ AUTHOR INFORMATION

Corresponding Author

*E-mail: skonar@iiserb.ac.in.

Notes

The authors declare no competing financial interest.

■ ACKNOWLEDGMENTS

S.B. thanks IISER Bhopal for a Ph.D. fellowship. H.S.J. thanks IISER Bhopal for a postdoctoral fellowship. A.A. acknowledges CSIR for their JRF fellowship. S.K. thanks DST, Government of India (Project SR/FT/CS-016/2010), and IISER Bhopal for generous financial and infrastructural support.

■ DEDICATION

Dedicated to Prof. Vinod K. Singh on receiving Padma shri, a prestigious civilian award of India.

■ REFERENCES

(1) (a) Gatteschi, D.; Sessoli, R.; Villain, J. *Molecular Nanomagnets*; Oxford University Press: Oxford, U.K., 2006. (b) Gatteschi, D.; Sessoli, R. *Angew. Chem., Int. Ed.* **2003**, *42*, 268–297. (c) Leuenberger, M. N.; Loss, D. *Nature* **2001**, *410*, 789–793. (d) Stone, R. *Science* **2009**, *325*, 1336–1337. (e) Wernsdorfer, W.; Sessoli, R. *Science* **1999**, *284*, 133–135.

(2) (a) Evangelisti, M.; Brechin, E. K. *Dalton Trans.* **2010**, *39*, 4672–4676. (b) Evangelisti, M.; Luis, F.; de Jongh, L. J.; Affronte, M. *J. Mater. Chem.* **2006**, *16*, 2534–2549.

(3) (a) Evangelisti, M.; Roubeau, O.; Palacios, E.; Camon, A.; Hooper, T. N.; Brechin, E. K.; Alonso, J. J. *Angew. Chem., Int. Ed.* **2011**, *50*, 6606–6609. (b) Lorusso, G.; Palacios, M. A.; Nichol, G. S.; Brechin, E. K.; Roubeau, O.; Evangelisti, M. *Chem. Commun.* **2012**, *48*, 7592–7594.

(4) (a) Karotsis, G.; Evangelisti, M.; Dalgarno, S. J.; Brechin, E. K. *Angew. Chem., Int. Ed.* **2009**, *48*, 9928–9931. (b) Langley, S. K.; Chilton, N. F.; Moubaraki, B.; Hooper, T.; Brechin, E. K.; Evangelisti, M.; Murray, K. S. *Chem. Sci.* **2011**, *2*, 1166–1169. (c) Shi, P. F.; Zheng, Y. Z.; Zhao, X. Q.; Xiong, G.; Zhao, B.; Wan, F. F.; Cheng, P. *Chem.—Eur. J.* **2012**, *18*, 15086–15091. (d) Sibille, R.; Mazet, T.; Malaman, B.; Francois, M. *Chem.—Eur. J.* **2012**, *18*, 12970–12973. (e) Wu, M.; Jiang, F.; Kong, X.; Yuan, D.; Long, L.; Al-Thaibati, S. A.; Hong, M. *Chem. Sci.* **2013**, *4*, 3104–3109. (f) Zhang, Z. M.; Pan, L. Y.; Lin, W. Q.; Ling, J. D.; Guo, F. S.; Chen, Y. C.; Liu, J. L.; Tong, M. L. *Chem. Commun.* **2013**, *49*, 8081–8083. (g) Hou, Y. L.; Xiong, G.; Shi, P. F.; Cheng, R. R.; Cui, J.-Z.; Zhao, B. *Chem. Commun.* **2013**, *49*, 6066–6068. (h) Guo, F. S.; Chen, Y. C.; Liu, J. L.; Leng, J. D.; Meng, Z. S.; Verbel, P.; Orendac, M.; Tong, M. L. *Chem. Commun.* **2012**, *48*, 12219–12221. (i) Chang, L.-X.; Xiong, G.; Wang, L.; Cheng, P.; Zhao, B. *Chem. Commun.* **2013**, *49*, 1055–1057. (j) Chen, Y. C.; Guo, F. S.; Zheng, Y. Z.; Liu, J. L.; Leng, J. D.; Tarasenko, R.; Orendac, M.; Prokleska, J.; Sechovsky, V.; Tong, M. L. *Chem.—Eur. J.* **2013**, *19*, 13504–13510. (k) Colacio, E.; Ruiz, J.; Lorusso, G.; Brechin, E. K.; Evangelisti, M. *Chem. Commun.* **2013**, *49*, 3845–3847. (l) Guo, F. S.; Leng, J. D.; Liu, J. L.; Meng, Z. S.; Tong, M. L. *Inorg. Chem.* **2012**, *51*, 405–413. (m) Guo, F. S.; Chen, Y. C.; Mao, L. L.; Lin, W. Q.; Leng, J. D.; Tarasenko, R.; Orendac, M.; Prokleska, J.; Sechovsky, V.; Tong, M. L. *Chem.—Eur. J.* **2013**, *19*, 14876–14889. (n) Lorusso, G.; Sharples, J. W.; Palacios, E.; Roubeau, O.; Brechin, E. K.; Sessoli, R.; Rossin, A.; Tuna, F.; Mclnnes, E. J. L.; Collison, D.; Evangelisti, M. *Adv. Mater.* **2013**, *25*, 4653–4656. (o) Goswami, S.; Adhikary, A.; Jena, H. S.; Konar, S. *Dalton Trans.* **2013**, *42*, 9813–9817. (p) Biswas, S.; Jena, H. S.; Goswami, S.; Sanda, S.; Konar, S. *Cryst. Growth Des.* **2014**, *14*, 1287–1295. (q) Adhikary, A.; Jena, H. S.; Khatua, S.; Konar, S. *Chem.—Asian. J.* **2014**, *9*, 1083–1090. (r) Zheng, Y.-Z.; Zhou, G.-J.; Zhenga, Z.; Winpenny, R. E. P. *Chem. Soc. Rev.* **2014**, *43*, 1462–1475. (s) Adhikary, A.; Sheikh, J. A.; Biswas, S.; Konar, S. *Dalton Trans.* **2014**, DOI: 10.1039/C4DT00540F.

(5) (a) Biswas, S.; Adhikary, A.; Goswami, S.; Konar, S. *Dalton Trans.* **2013**, *42*, 13331–13334. (b) Goswami, S.; Adhikary, A.; Jena, H. S.; Biswas, S.; Konar, S. *Inorg. Chem.* **2013**, *52*, 12064–12069.

(6) Wang, L.; Gu, W.; Deng, X. J.; Zheng, L. F.; Liao, S. Y.; Zhang, M.; Yang, L. Y.; Liu, X. *Aust. J. Chem.* **2011**, *64*, 1373–1382.

(7) (a) Torquato, S.; Jiao, Y. *Nature* **2009**, *460*, 877–879. (b) Damasscenco, P. F.; Engel, M.; Glotzer, S. C. *ASC Nano* **2012**, *6*, 609–614. (c) Torquato, S.; Jiao, Y. *Phys. Rev. E* **2009**, *80*, 041104–041125. (d) Song, W. M.; Matteo, T. D.; Aste, T. *Phys. Rev. E* **2012**, *85*, 046115.

(8) Spek, A. L *PLATON: A Multipurpose Crystallographic Tool*; Utrecht University: Utrecht, The Netherlands, 2001.

(9) Blatov, V. A. *Reticular Chemistry Structure Resource*.

(10) (a) Zhao, L.; Xue, S.; Tang, J. *Inorg. Chem.* **2012**, *51*, 5994–5996. (b) Gass, I. A.; Moubaraki, B.; Langley, S. K.; Batten, S. R.; Murray, K. S. *Chem. Commun.* **2012**, *48*, 2089–2091.

(11) Sessoli, R. *Angew. Chem., Int. Ed.* **2012**, *51*, 43–45.

(12) (a) Shi, P. F.; Xiong, G.; Zhao, B.; Zhang, Z. Y.; Cheng, P. *Chem. Commun.* **2013**, *49*, 2338–2340. (b) Liu, Y.; Chen, Z.; Ren, J.; Zhao, X. Q.; Cheng, P.; Zhao, B. *Inorg. Chem.* **2012**, *51*, 7433–7435.